Safety factor influence on the edge E x B velocity establishment in tokamak plasmas.

Robin Varennes, Laure Vermare, Xavier Garbet, P Hennequin, G. Dif-Pradalier, Yanick Sarazin, Virginie Grandgirard, Olivier Panico, Peter Donnel, K. Obrejan

Safety factor influence on the edge $E \times B$ velocity establishment in tokamak plasmas.

R. Varennes[1], L. Vermare[1], X. Garbet[2,3], P. Hennequin[1] G. Dif-Pradalier[2],
Y. Sarazin[2], V. Grandgirard[2], O. Panico[1], P. Donnel[2], K. Obrejan[2]
[1]*LPP, CNRS, Ecole polytechnique, 91128 Palaiseau, France.*
[2]*CEA, IRFM, F-13108 Saint-Paul-Lez-Durance, France.*
[3]*Nanyang Technological University, 637371 Singapore.*

This study is motivated by experiments on Tore Supra and WEST tokamaks where a deepening of the radial electric field near the edge is observed when the safety factor decreases. Flux-driven global simulations of Ion Temperature Gradient (ITG) turbulence recover qualitatively the trend observed in the experiments, i.e. the $E \times B$ velocity increases when decreasing the safety factor. From these simulations, multiple clues point out the role of turbulence in the establishment of the radial electric field even though the linear growth rate increases with the safety factor. The proposed mechanism to elucidate this phenomenon, backed up by a reduced model, is that the neoclassical friction - particularly sensitive to the safety factor - effectively damps the effect of the turbulent drive.

I. INTRODUCTION

The onset and sustainment of edge transport barriers in tokamak plasmas, which greatly improve the energy confinement by reducing turbulent transport, are attributed to strongly depend on the shear of the edge $E \times B$ transverse flow [1]. The mechanisms that control this flow, which is governed by the radial electric field E_r, are therefore a major topic of research in the fusion community. The physics governing the establishment of the radial electric field - particularly the well at the plasma edge - is not fully understood especially in the L-mode and towards the L-H transition. In this context, experimental observations on the Tore Supra [2] and the WEST [3] tokamaks during ohmic and low power discharges have demonstrated a deepening of the transverse plasma velocity shear, governed by the radial electric field, near the edge with increasing plasma current. These experiments constitute a great framework to study the impact of the plasma current on the radial electric field, especially when considering the critical role this key parameter plays in overall confinement properties. In the first place, most scaling laws indicate that the energy confinement time is increasing, almost linearly, with the plasma current in the H-mode operational regime. In addition, the power threshold for the transition toward H-mode, usually considered independent of the plasma current for a wide selection of tokamaks [4], has actually been observed to depend on I_P in the ASDEX-Upgrade tokamak in the low-density branch [5]. Indeed, various mechanisms are involved in the plasma current role on the stability and dynamics of the plasma. It sets the poloidal component of the magnetic field and therefore the safety factor, which in turn is involved in transit times along field lines and orbit widths. These factors are instrumental in a large variety of neoclassical and turbulent physical processes. For instance, the safety factor's influence on the bounce frequency of trapped particles is critical in understanding neoclassical transport. Additionally, its effect on turbulent transport, mediated by the linear growth rate of electrostatic instabilities, further underlines its significance.

In this paper, an identification of mechanisms leading to the experimental plasma current dependence of the edge $E \times B$ velocity profile are addressed using gyrokinetic simulations of ITG driven turbulence. The experimental trend is recovered, i.e. the amplitude of the edge radial electric field increases when the safety factor decreases. However, this effect is comparatively milder than the one observed in experiments. A tentative reduced model is proposed to extract the main safety factor dependencies of the equilibrium radial electric field.

The remainder of this paper is organized as follows. In Section II, experimental results from the Tore Supra tokamaks are presented and act as a reference for the following numerical study. Section III exposes the results of the gyrokinetic simulations of ITG-driven turbulence performed with the global full-f code GYSELA. In Section IV is proposed a reduced model for the equation that governs the equilibrium radial electric field. In Section V is discussed the results and remaining open questions.

II. EXPERIMENTAL EVIDENCE OF PLASMA CURRENT INFLUENCE ON THE RADIAL ELECTRIC FIELD

The deepening of the E_r profile at the edge when increasing the plasma current has been observed experimentally both in the Tore Supra [2] and the WEST [3] tokamaks. These observations have been obtained during Ohmic plasmas through the measurement of the velocity of density fluctuations using a Doppler Back-Scattering (DBS) diagnostic [6, 7] and recently confirmed in moderately heated plasmas in WEST. This microwave technique selects spatial scale ($k_\perp$) density fluctuations and gives access to their mean velocity, labeled V_{DBS}, in the bi-normal direction (normal both to the magnetic field lines and to the radial direction and referred as "perpendicular" in the following). It reads $V_{\mathrm{DBS}} = V_{\mathrm{E}} + V_{\mathrm{ph}}$ where $V_{\mathrm{E}} \approx -E_r/B$ is the mean electric drift velocity

and $V_{\rm ph}$ is the so-called phase velocity of the fluctuations since it is related to their own velocity in the plasma frame. This "phase velocity" is commonly considered negligible with respect to the mean plasma velocity at the plasma edge where the $V_{\rm E}$ velocity can reach a high value. Note however that it can become significant in some radial regions with weaker $V_{\rm E}$ [8].

Dedicated Ohmic plasma experiments were performed both in the Tore Supra and WEST tokamak to study the impact of the safety factor on the plasma flow velocity at the edge. The main difference between these two experiments comes from the plasma shape: circular in Tore Supra while diverted in WEST. In the context of comparison with gyrokinetic simulation, the focus is given in this paper on circular plasma experiments. Tore Supra discharges have been performed to study the effect of parallel flow in the Scrape-Off Layer [2] by moving the plasma/wall contact point from the top to the bottom of the outboard limiter. Note that the $B \times \nabla B$ drift always points down in Tore Supra as well as in WEST. In addition, in each configuration (depending on the position of the contact point), a safety factor scan was performed by varying the plasma current I_P. This way, the edge safety factor has been varied from $q_{95} = 3.2$ to $q_{95} = 4.5$ while keeping the density constant.

Fig.1 displays the radial profile of the perpendicular velocity profiles of the density fluctuations during the I_P scan in a bottom contact point configuration. The measured edge velocity is observed to increase significantly in absolute value when increasing the plasma current. As the phase velocity can be considered negligible in this experiment, it suggests a clear increase of the radial electric field with I_P in the edge region. During this discharge, no significant evolution of the ion temperature T_i profile (measured using Charge eXchange Recombination Scattering (CXRS) at two times during the I_P-ramp) is observed between $r/a = [0.2 - 0.9]$. Unfortunately, no measurements are available for T_i between $r/a = [0.9 - 1]$ where the peak of velocity variation is observed. Note that the same trend on E_r is observed in the top configuration as well as during a discharge with a limiter configuration - not dedicated to the velocity measurements and with a low radial resolution.

These observations have been confirmed in WEST plasma, both in Lower Single Null and Upper Single Null configurations [3] suggesting 1) that the sensitivity of the mean flow velocity to the safety factor is robust during Ohmic and low power discharges and 2) that the physics of the X-point and of the plasma shape are not the main ingredients in the underlying mechanisms responsible for the observed plasma current sensitivity. These elements are the motivation for the numerical work of the next section.

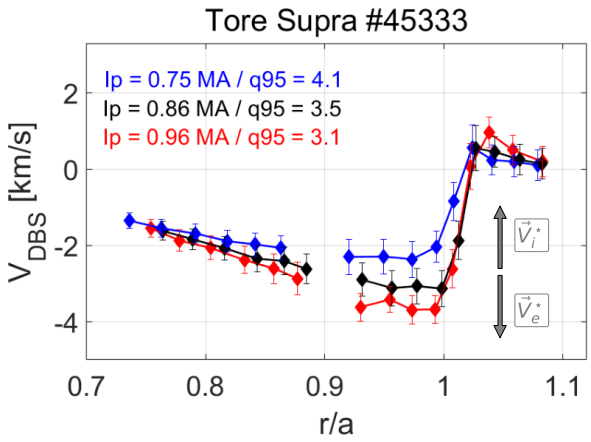

FIG. 1: Perpendicular velocity profiles measured during the I_P ramp-up of Tore Supra discharge #45333, measured with the DBS diagnostic (positive/negative values point to the ionic/electronic diamagnetic velocity direction respectively).

III. SAFETY FACTOR IMPACT ON $E \times B$ VELOCITY IN GYROKINETIC SIMULATIONS

In this section, the safety factor impact on the radial electric field in gyrokinetic simulations performed with the GYSELA code [9] is investigated. For this purpose, a reference flux-driven simulation of ITG driven turbulence, described in [10] and denominated $q_{\rm ref}$, is considered. This case corresponds to the high collisionality experimental discharge (#45511) of a collisionality scan performed in Tore Supra [8] and exhibits realistic shapes of thermodynamical gradients (not related to the experimental discharges shown in Section II). This reference case is performed with adiabatic electrons and only one ion species. It includes a limiter [11] which acts as a heat sink, resulting in steep gradients able to spread turbulence from the limiter to the core [10]. In addition, a carefully tailored heat source in the core keeps the temperature gradient profile quasi-steady. From this reference case, two other cases, denominated $q_{\rm ref} \times 0.5$ and $q_{\rm ref} \times 1.5$ have been run where the safety factor profile from the $q_{\rm ref}$ case have been multiplied by 0.5 and 1.5 respectively. The resulting safety factor profiles for each simulation are displayed in Fig.2. Note that safety factor values under unity are allowed as these cases are electrostatic, i.e. not subject to MHD instabilities. This homothety on the reference q profile allows to assess the sole effect of the safety factor while keeping the magnetic shear unchanged coherently with the experiments. Indeed, magnetic shear is expected to impact the linear growth rate [12] and, as such, the poloidal Reynolds stress. In GYSELA, the collisionality $\nu^\star = \nu_i \frac{qR_0}{V_{\rm th}\varepsilon^{3/2}}$ is an input of the code, which is here left unchanged between each simulation. In other words, the collision frequency adapts in order to compensate for the linearity with q

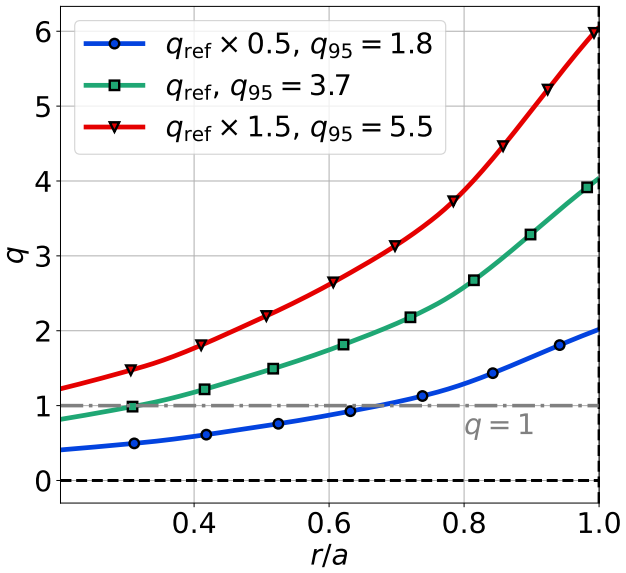

FIG. 2: Radial profile of safety factor in each simulated case.

of the collisionality such that the product $\nu_i q$ is equal in each simulation. Thus, neoclassical regimes are the same in each case. From this perspective, these simulations do not effectively match experimental conditions in which $\nu^\star$ varies with the plasma current. Note that cases were run where both the safety factor and collisionality were adjusted in such a way that the collision frequency remained constant. These adjustments did not change qualitatively the results described below in the considered collisionality range $0.1 < \nu_\star < 1$.

The overall dynamic of the transverse $E \times B$ velocity for each case is captured in Fig.3 showing the spatiotemporal evolution of this quantity. As already pointed out in [13, 14], diminishing q leads to the establishment of quasi-static zonal structures known as staircases. Conversely, increasing the value of q leads to higher frequency events, particularly Geodesic Acoustic Modes driven by turbulence, which exhibit a significant decrease in damping as q increases. Both of these dynamics are powered by turbulent processes and are expected to be a key element in the flow establishment. In Fig.4 is displayed the radial profile of the edge poloidal $E \times B$ velocity averaged on 10^5 reference cyclotron periods ω_{c0}^{-1} in the equilibrium state. The experimental trend is recovered, i.e. edge $|V_{\rm E}|$ increases when the safety factor decreases. Note that the temperature gradients are similar in these three simulations in the radial span $0.6 < r/a < 0.95$. The effect of thermodynamical gradients on $V_{\rm E}$ can then be discarded. In addition, the same simulations have been run where all the toroidal modes n of the electric potential except the axisymmetric one $n = 0$ have been artificially set to zero. This method is used to obtain simulations where most of the turbulence is suppressed and neoclassical processes prevail. The time evolution of edge V_E for the turbulent and non-turbulent versions of the cases $q_{\rm ref} \times 0.5$ and $q_{\rm ref} \times 1.5$ is depicted in Fig.5 It reveals a significantly larger gap in the amplitude of V_E between low and high safety factor cases when turbulence is accounted for, indicating that the effect on V_E cannot be explained by neoclassical processes only.

An important remark is that the time to reach the equilibrium state increases when diminishing the safety factor, as somewhat perceivable from Fig.3. In practice, the equilibrium in the simulation case $q_{\rm ref} \times 0.5$ is reached at about $t = 150000[\omega_{c0}^{-1}]$ which roughly corresponds to $1ms$. This feature corroborates the fact that both the linear growth rate [12, 15] and the collisional friction increase with q.

In these simulations, the increase of $V_{\rm E}$ with q^{-1} is mild - compared with experiments - and appears to saturate at high safety factor values. This saturation is coherent with the numerical work done in [12] in which a safety factor scan with the linear growth rate has been performed in gyrofluid simulations of Trapped Electron Modes turbulence. Indeed, as detailed in the next section, the turbulent contribution to $V_{\rm E}$ scales with the Reynolds stress divergence, itself increasing with the linear growth rate. This is also the case in the presented simulations, as shown in Fig.6a that displays the radial profile of the Reynolds stress divergence coarse-grained radially and temporally $\langle \nabla \cdot \Pi \rangle_{\rm CG}$. Accordingly, the turbulent intensity $\mathcal{I} = \sqrt{\left|\frac{e\tilde{\phi}}{T_e}\right|^2}$ (where $\tilde{\phi}$ is the fluctuating part of the electric potential and T_e the electron temperature) is also witnessed to grow with the safety factor in our simulation, as shown in Fig.6b. This quantity is a proxy for the Reynolds stress that is comparable to the experiments. The significant gap between experimental edge turbulent intensity, typically around 10%, and the few percent values observed in these simulations is a consistent feature across all gyrokinetic codes. This disparity is partly explained by the fact that some drives are missing (i.e. the TEM, ETG and electromagnetic turbulence in this work) and suggests that the turbulent contribution is under-estimated in these simulations. An important question remains: if the turbulent contribution to $V_{\rm E}$ can explain the experimental results, why does $|V_{\rm E}|$ increase when the safety factor decreases? In other words, why does the turbulent contribution actually increase when turbulence is weaker? The next section aims to elucidate this conundrum thanks to a simple reduced model.

IV. REDUCED MODEL FOR EQUILIBRIUM $E \times B$ VELOCITY

The electrostatic version of the gyrokinetic code GYSELA [9] with adiabatic electrons solves the Fokker-Plank equation and the Poisson equation. The Fokker-Plank equation describes the evolution of the gyrocenter

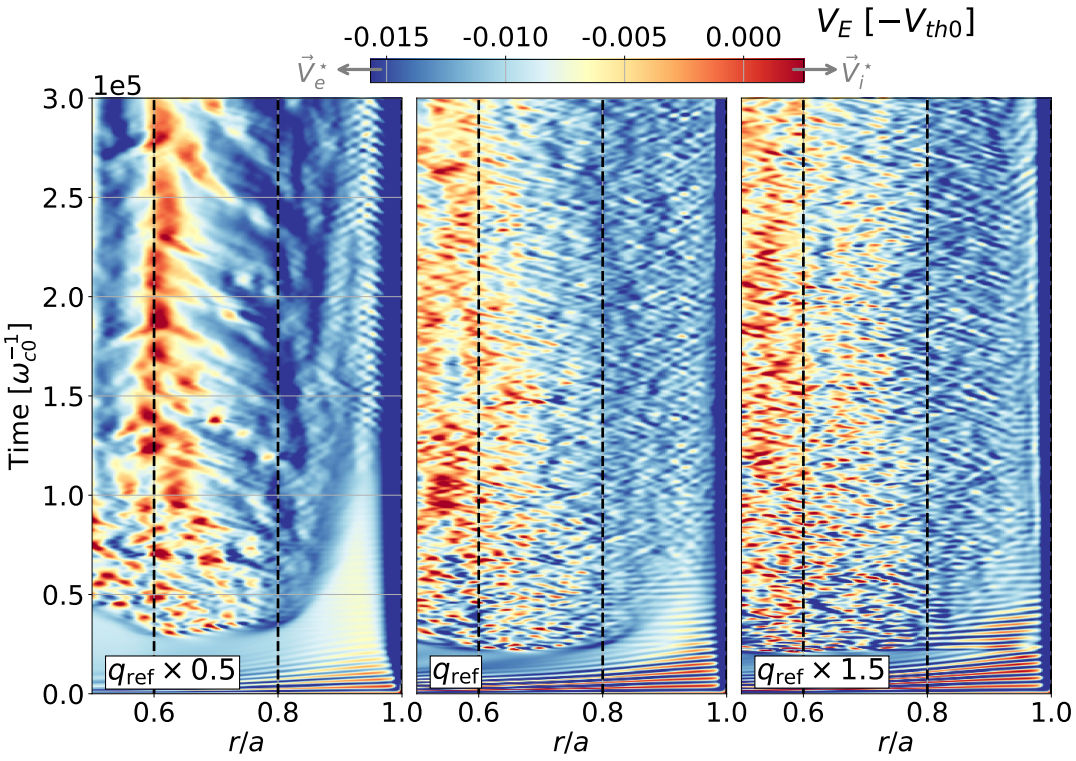

FIG. 3: Spatio-temporal evolution of the transverse $E \times B$ velocity, normalized to the opposite thermal ion velocity at midradius V_{th0}, for each simulated case.

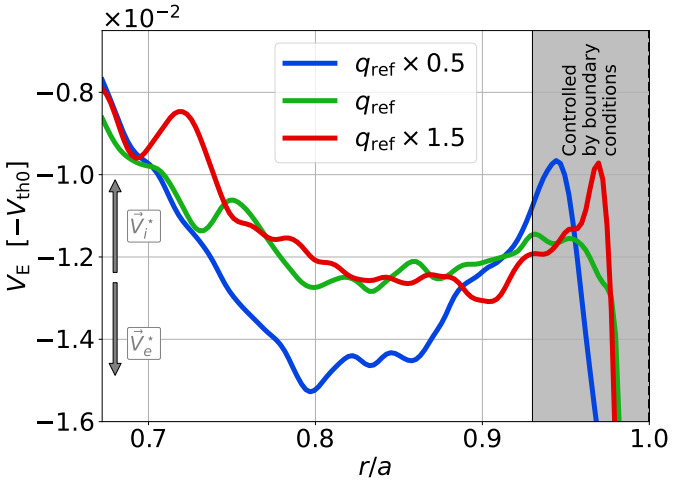

FIG. 4: Radial profile of V_{E} (oriented in the ion diamagnetic drift direction) time-averaged between $160\,000 < t[\omega_{c0}^{-1}] < 300\,000$.

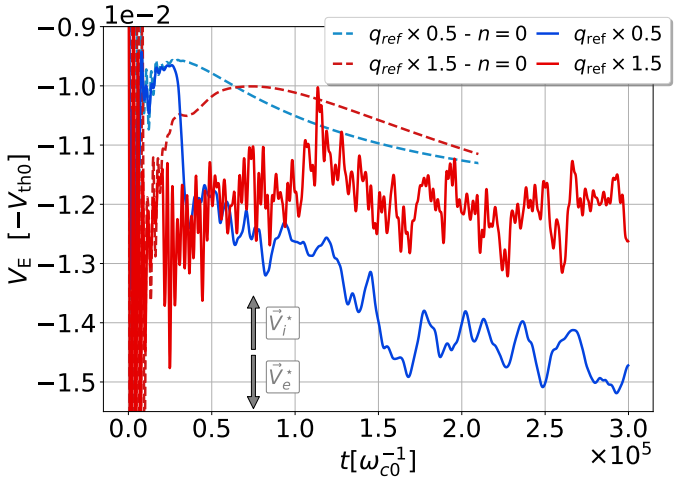

FIG. 5: Temporal evolution of V_{E} (oriented in the ion diamagnetic drift direction) average in the radial range $0.76 < r/a < 0.86$. The cases referred to as "$n = 0$" are non-turbulent and dominated by neoclassical effects.

distribution function $\bar{F}_s$ of each species s and reads

$$\frac{\partial \bar{F}_s}{\partial t} + \frac{\mathrm{d}\mathbf{x}_G}{\mathrm{d}t} \cdot \boldsymbol{\nabla} \bar{F}_s + \frac{\mathrm{d}v_{G\parallel}}{\mathrm{d}t} \frac{\partial \bar{F}_s}{\partial v_{G\parallel}} = \mathcal{C}(\bar{F}_s) + \mathcal{S}_s \qquad (1)$$

where $\mathcal{C}$ is a collision operator [16] and $\mathcal{S}_s$ a heat source.

Considering only one ion species, the electrostatic quasi-neutrality equation, in the case of adiabatic electrons and in the limit of long wavelengths (with respect

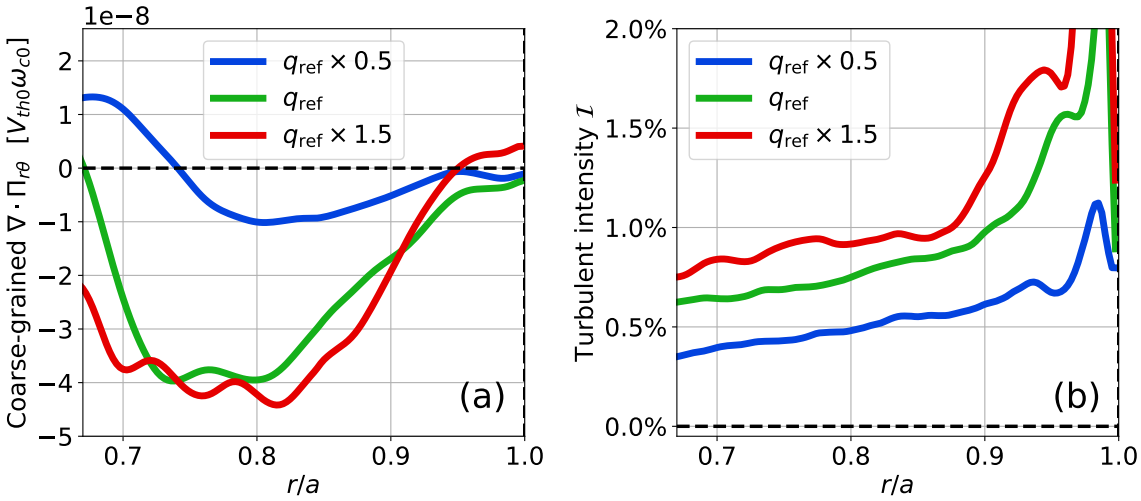

FIG. 6: (a) Radial profile of simulations, averaged on 100 000 ω_{c0}^{-1}, of (a) the Reynolds stress divergence with a radial sliding average with a $\sim 40\rho_i$ window and of (b) the turbulent intensity.

to the thermal ion Larmor radius), reads:

$$\frac{e^2 n_0}{T_0}\left[\phi - \langle\phi\rangle\right] - \nabla_\perp \cdot \left[\frac{m n_0}{B_0^2}\nabla_\perp \phi\right] \tag{2}$$

$$= \iint \frac{2\pi B_\parallel^\star}{m} dv_{G\parallel} d\mu \mathcal{J}(\bar{F} - \bar{F}_{\rm eq}) \tag{3}$$

where $\langle . \rangle$ denotes a flux-surface average, $\mathcal{J}$ is the gyroaverage operator, ϕ is the electric potential, T_0 is the initial electron temperature, e the ion charge, B_0 the magnetic field amplitude on the magnetic axis, n_0 is the initial electron density, m is the ion mass and $B_\parallel^\star$ is the Jacobian of the phase space coordinate transform.

From these equations and with the Padé approximation for the gyroaverage operator $\mathcal{J}[\phi] \simeq \phi + \frac{1}{2}\boldsymbol{\nabla}\cdot\left(\frac{m\mu}{e^2 B}\boldsymbol{\nabla}_\perp\phi\right)$, one can obtain an equation describing evolution on the transverse $E\times B$ velocity, i.e. the radial electric field E_r, that reads

$$\frac{m n_0}{B_0}\frac{\partial}{\partial t}\left(V_{\rm E} + \frac{1}{2}\frac{\omega_{c0}}{n_0 m}\frac{\partial\langle P_\perp\rangle}{\partial r}\right) - \langle J_r\rangle = RHS \tag{4}$$

where ω_{c0} is a reference cyclotron frequency, $V_{\rm E} = \langle\nabla_\perp\phi\rangle/B_0 = -E_r/B_0$ and $P_\perp \equiv \int d^3 v \mu B \bar{F}$ is the ion perpendicular pressure. The radial current $\langle J_r\rangle$ is driven by magnetic and electric velocity drifts. The RHS contains lower order terms, including the effect of heat source and gyroaverage of the collision operator. It is set to zero in the following. The radial profile of the terms appearing in Eq(4) in the presented gyrokinetic simulations are presented in Fig.7. It appears that this conservation equation is met by GYSELA up to the numerical precision of the code. While this "integrated vorticity" equation is nothing else than the continuity equation integrated radially, the authors stress that seemingly proper density conservation does not guarantee that Eq(4) is fulfilled. Indeed, during this work, it has been identified cases where small numerical disparity accumulated along the radial direction which led to Eq(7) being unfulfilled, resulting in a wrong radial electric field. In this exact equation, the current can be split into a neoclassical component $J_{\rm neo}$, that comes from collisional processes, and a turbulent component $J_{\rm turb}$ that comes from instabilities driven by thermodynamical gradients.

They can formally be written as moments of the distribution function F as

$$J_{\rm neo} = e\Big\langle \int \left((\boldsymbol{v_D}\cdot\boldsymbol{\nabla}r) + \langle \boldsymbol{v}_{\rm E}\cdot\boldsymbol{\nabla}r\rangle_\varphi\right) F d^3\boldsymbol{v}\Big\rangle_{FS} \tag{5}$$

$$J_{\rm turb} = e\Big\langle \int \left((\boldsymbol{v}_{\rm E}\cdot\boldsymbol{\nabla}r) - \langle \boldsymbol{v}_{\rm E}\cdot\boldsymbol{\nabla}r\rangle_\varphi\right) F d^3\boldsymbol{v}\Big\rangle_{FS} - \frac{m}{2eB_0^2}\frac{\partial^2\langle P_\perp\rangle}{\partial t\partial r} \tag{6}$$

where $\boldsymbol{v_D}$ and $\boldsymbol{v}_{\rm E}$ are respectively the gyrocenter electric and magnetic drift velocities. It can be shown that the time derivative in Eq(6) is the divergence of a heat-flux contributing to the diamagnetic corrections for the Reynolds stress. The currents expressed in Eq(5) and Eq(6) do not readily reveal their dependency on the safety factor.

From now on, reduced models will be used for these currents in order to predict the safety factor effect on the radial electric field evolution.

Regarding the neoclassical current $J_{\rm neo}$, many studies [17–21] propose the following approximative frictional form:

$$J_{\rm neo} = -\frac{m n_0}{B_0}\nu_{\rm neo}\left(V_{\rm P} - V_{\rm P,neo}\right) \tag{7}$$

where $\nu_{\rm neo}$ is the neoclassical friction that sets the rate at which the poloidal velocity $V_{\rm P}$ reaches its neoclassical prediction $V_{\rm P,neo} = k\frac{\partial_r T}{eB_0}$ (where k is a number that depends on the collisional regime). From the authors' knowledge, the dynamic structure of Eq(7) has never

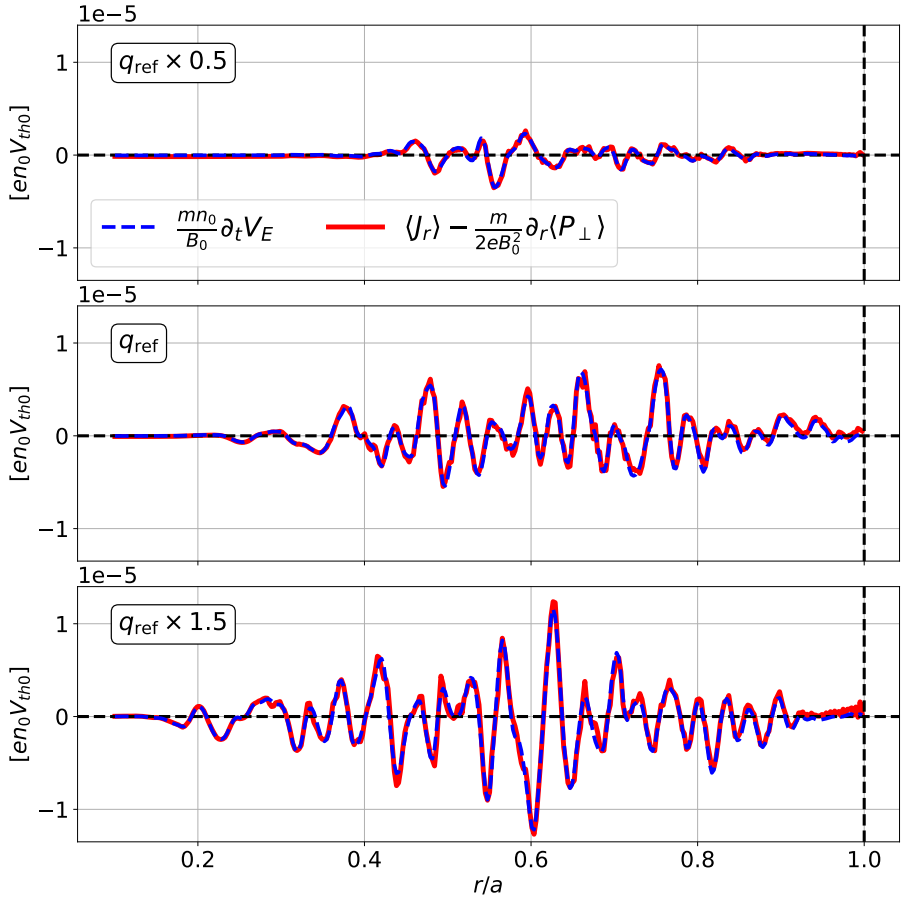

FIG. 7: Radial profile of integrated vorticity conservation Eq(4) terms.

been assessed in gyrokinetic simulations. Indeed, while the equilibrium velocity $V_{\rm P,neo}$ has been recovered in multiple codes, including GYSELA [22], the neoclassical friction $\nu_{\rm neo}$ still lacks a validation with first-principle codes. In addition, while $V_{\rm P,neo}$ is derived from exact equations, the neoclassical friction predictions are obtained by means of several approximations. A numerical identification of this friction rate appears difficult for the reasons detailed in Appendix A, where an attempt has been made with GYSELA. Results are encouraging regarding the frictional structure of Eq(7) and the monotonic increase of $\nu_{\rm neo}$ with the safety factor. When committing to this approximation, one can express the poloidal velocity through the force balance equation, which is always verified in GYSELA simulations. It reads

$$V_{\rm P} = V_{\rm E} + \frac{\varepsilon}{q}V_{\rm T} + \frac{\partial_r(n_0 T)}{n_0 e B_0} \tag{8}$$

where $\varepsilon = r/a$, T is the ion temperature and V_T is the mean toroidal velocity. This equation allows to cast the neoclassical current $J_{\rm neo}$ as a function of the electric drift $V_{\rm E}$.

Regarding the turbulent current $J_{\rm turb}$, the incompressibility constraint allows the following expression:

$$J_{\rm turb} = -\frac{mn_0}{B_0}\nabla\cdot\bar{\bar{\Pi}}_{\rm turb} \tag{9}$$

where the (r,θ) component of the poloidal Reynolds stress $\bar{\bar{\Pi}}_{\rm turb} = \bar{\bar{\Pi}}^{\rm E\times B}_{\rm turb} + \bar{\bar{\Pi}}^{\rm dia}_{\rm turb}$ is the sum of the electric and the diamagnetic Reynolds stresses. The approximation of this turbulent current has been assessed in our GYSELA simulations. In Fig.8 is displayed the radial profiles of both $J_{\rm turb}$ and $-\frac{mn_0}{B_0}\nabla\cdot\bar{\bar{\Pi}}_{\rm turb}$ at an instantaneous time for the $q_{\rm ref}\times 0.5$ and $q_{\rm ref}\times 1.5$ cases. A good agreement is found on both the amplitude and the phase of these two quantities, giving us confidence in this approximation. Note that the diamagnetic tensor is essential to recover this equality. Indeed, as detailed in [23], the diamagnetic tensor $\bar{\bar{\Pi}}^{\rm dia}_{\rm turb}$ is in phase and about two times larger than its $E\times B$ counterpart $\bar{\bar{\Pi}}^{\rm E\times B}_{\rm turb}$. Under these approximations, the equilibrium $E\times B$ poloidal velocity is

$$V_{\rm E,eq} = (k-1)\frac{\partial_r T}{eB_0} - \frac{\nabla\cdot\bar{\bar{\Pi}}_{\rm turb}}{\nu_{\rm neo}} - \frac{\varepsilon}{q}V_{\rm T} - \frac{T}{eB_0}\partial_r \ln n_0 \tag{10}$$

At constant thermodynamical profiles, this equation shows that the radial electric field dependence on the

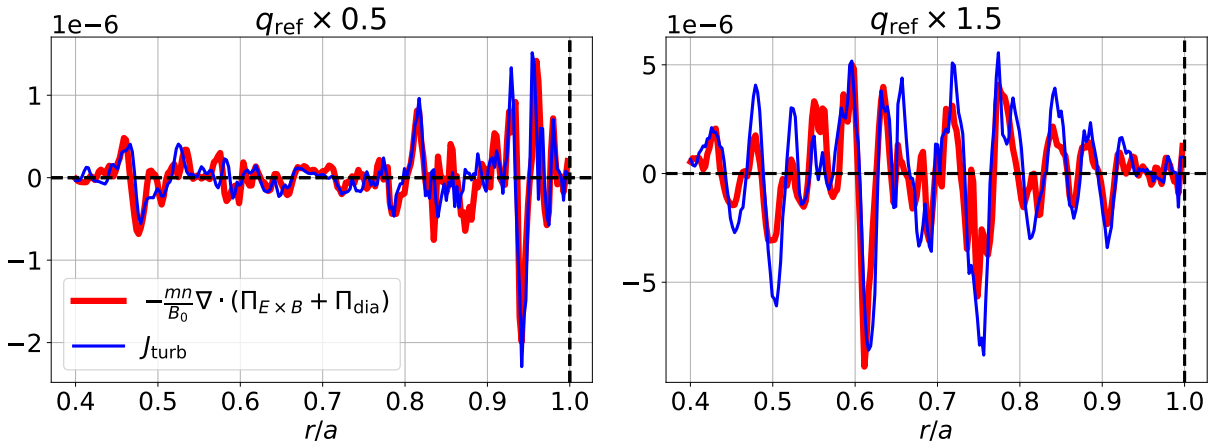

FIG. 8: Instantaneous radial profiles of J_{turb} and $-\frac{mn_0}{B_0}\bar{\bar{\Pi}}_{\mathrm{turb}}$ in the $q_{\mathrm{ref}} \times 0.5$ and $q_{\mathrm{ref}} \times 1.5$ simulated cases.

safety factor comes from two terms. On the one hand, there is the term $\nabla \cdot \bar{\bar{\Pi}}_{\mathrm{turb}}/\nu_{\mathrm{neo}}$ which indicates that the turbulent contribution to $V_{\mathrm{E,eq}}$ is damped by the collisional friction. This contribution is particularly interesting as theoretical scalings of ν_{neo} show a strong sensitivity to the safety factor - either linear or quadratic depending on the collisional regime - while the turbulent source is only weakly affected in our simulation as already documented in many publications [12–15, 24, 25]. This might account for why a seemingly less turbulent case can actually have a significant turbulent contribution to V_{E}. On the other hand, there is the contribution of the toroidal velocity V_{T}. While in experiments one could expect that V_{T} results from a competition between neoclassical processes and turbulence [26], here the presented simulations are performed in an axisymmetric magnetic configuration so only the turbulence contributes. Even if the associated contribution to V_{E} is mild in simulations, interestingly the toroidal velocity appears to have a non-monotonic trend with the safety factor. Preliminary observations point out the interactions between the plasma and the limiter. Such a mechanism is beyond the scope of this study but is worth considering for future studies as the toroidal velocity in these GYSELA simulations is far from experimental conditions.

V. DISCUSSION AND OPEN QUESTIONS

This study provides an assessment of the role of the safety factor in the establishment of the edge radial electric field in a tokamak plasma. Numerical simulations of turbulence driven by ITG were performed with the gyrokinetic code GYSELA to investigate an experimental observation conducted on Tore Supra and WEST tokamaks, where a deepening of the radial electric field near the edge was observed as the safety factor decreased. The same trend is recovered in simulations and the resulting radial electric field appears correlated with the turbulent drive, i.e. the Reynolds stress divergence, while the neoclassical effects alone appears negligible. As already documented in other numerical studies, the amplitude of this turbulent drive increases with the safety factor, which seems paradoxical as the overall turbulent contribution actually decreases. An explanation is proposed based on a reduced model which is derived from exact equations (in the adiabatic electrons framework) demonstrating that the radial electric field evolution is influenced by neoclassical and turbulent contributions. A reasonably good approximation for the turbulent contribution, backed up by the simulations presented in this study, is that it is proportional to the Reynolds stress divergence. However, the situation becomes more challenging when dealing with the neoclassical contribution. Indeed, many theoretical works [17–20] propose a frictional form for this contribution. This form is questionable considering its derivation comes from the non-turbulent case, among other limiting approximations. When one commits to this frictional form though, the resulting equilibrium radial electric field appears to be the sum of a pure neoclassical contribution - independant of the safety factor - and another term describing that the turbulent drive for the electric field is damped by collisional processes. While the turbulent drive, i.e. the turbulent Reynolds stress, mildly increases ($\propto q^{\sim 0.5}$) with the safety factor, the collisional damping increases substantially ($\propto q^{1-2}$). In consequence, this turbulent contribution could explain why diminishing the safety factor actually accounts for an increased radial electric field amplitude. In other words, a low safety factor allows for the presence of undamped turbulent contribution to the radial electric field. Some publications mentioning this contribution [21, 27] consider it small. While the presented simulations, indeed, do not fully capture the amplitude of the safety factor effect on the radial electric field as observed in experiments, one cannot overlook the fact that the measured turbulent intensity in experiments is consistently substantially higher than the one obtained in any simulation

code. The simulations of this study only include ITG turbulence, but one has to consider all turbulent drives for a realistic description. A more complete description would surely result in a more important turbulent drive and thus a stronger turbulent contribution to the radial electric field.

ACKNOWLEDGMENTS

This work has been carried out within the framework of the EUROfusion Consortium, funded by the European Union via the Euratom Research and Training Programme (Grant Agreement No 101052200 — EUROfusion). Views and opinions expressed are however those of the author(s) only and do not necessarily reflect those of the European Union or the European Commission. Neither the European Union nor the European Commission can be held responsible for them. This work was carried using HPC resources from GENCI, CCRT-TGCC and CINECA. This work was supported by funding from the European Union's Horizon 2020 research and innovation program under grant agreement no. 824158 (EoCoE II).

Appendix A: Poloidal neoclassical friction in GYSELA

An attempt is made in this work to numerically retrieve the neoclassical friction coefficient $\nu_{\rm neo}$ with GYSELA and to compare it with the predictions. To do this, the same approach as in [28] which allowed retrieval of the toroidal friction in a non-axisymmetric device was used. The idea is to initialize the poloidal velocity to different values in multiple simulations and extract the friction coefficient from the relaxation of this velocity. Compared to the toroidal friction, the problem is twofold. First, the friction coefficient is predicted to be in the $10^{-4}[\omega_{c0}]$ range, meaning that the whole relaxation phase occurs during the initial GAMs phase. Second, the poloidal velocity is not an input of the code. Still, an attempt is made by modifying $V_{\rm P}$ through the density gradient, affecting the diamagnetic velocity (with a weak impact on collisionality, which is not expected to significantly affect the results). The time evolution of $V_{\rm P}$ is displayed in Fig.9a, showing the fast relaxation. Fig.9b shows the link between this velocity and the exact neoclassical current defined in Eq(5), confirming that they are indeed proportional and gives confidence in the approximation of the fictional form Eq(7).

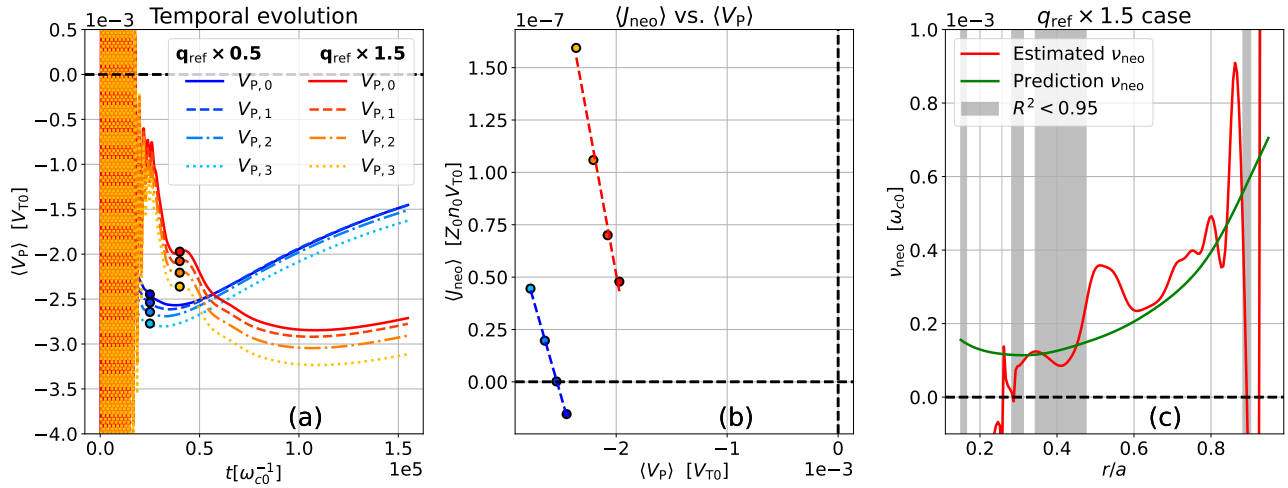

FIG. 9: (a) Temporal evolution averaged in $0.65 < r/a < 0.7$ of $V_{\rm P}$ for multiple GYSELA simulations with different initial $V_{\rm P}$ and safety factor. (b) Poloidal velocity and associated neoclassical current $J_{\rm neo}$. (c) Neoclassical friction $\nu_{\rm neo}$ estimated in the $q_{\rm ref} \times 1.5$ case vs. predictions from [29] (grey zones represents the radial coordinates where the linear regression is such that $R^2 < 0.95$).

The slope given by the linear regression is directly related to the neoclassical friction, for which the resulting radial profile for the $q_{\rm ref} \times 1.5$ case is plotted in Fig.9c and compared to the theoretical predictions from *Gianakon et al.* [29]. While noisy, the reconstructed friction is in fair agreement with the prediction. However this match is not retrieved in the $q_{\rm ref} \times 0.5$ case, and neither in the phase that follows the initial relaxation. The authors suggest that the model equation for $J_{\rm neo}$ lacks a key component: the parallel heat flux, as noted in [30]. This initial study of poloidal neoclassical friction is nonetheless comforting as it suggests that $J_{\rm neo}$ can indeed be expressed in a frictional form, and that this friction is an increasing function of the safety factor.

[1] K. H. Burrell et al. *Plasma Phys. Control. Fusion*, 31, 1989. doi:10.1088/0741-3335/31/10/012.

[2] P. Hennequin et al. *37th EPS Conference on Plasma Physics 2010, EPS 2010*, 1, 2010.

[3] L. Vermare et al. *Nucl. Fusion*, 62, 2021. doi: 10.1088/1741-4326/ac3c85.

[4] Y. R. Martin et al. *J. Phys.: Conf. Ser.*, 123, 2008. doi: 10.1088/1742-6596/123/1/012033.

[5] F. Ryter et al. *Nucl. Fusion*, 53, 2013. doi:10.1088/0029-5515/53/11/113003.

[6] P. Hennequin et al. *Review of Scientific Instruments*, 75, 2004. doi:10.1063/1.1787920.

[7] P. Hennequin et al. *Nucl. Fusion*, 46, 2006. doi: 10.1088/0029-5515/46/9/S12.

[8] L. Vermare et al. *Physics of Plasmas*, 18, 2011. doi: 10.1063/1.3536648.

[9] V. Grandgirard et al. *Computer Physics Communications*, 207, 2016. doi:10.1016/j.cpc.2016.05.007.

[10] G. Dif-Pradalier et al. *Commun Phys*, 5, 2022. doi: 10.1038/s42005-022-01004-z.

[11] E. Caschera et al. *J. Phys.: Conf. Ser.*, 1125, 2018. doi: 10.1088/1742-6596/1125/1/012006.

[12] R. E. Waltz et al. *Physics of Plasmas*, 4, 1997. doi: 10.1063/1.872228.

[13] P. Angelino et al. *Plasma Phys. Control. Fusion*, 48, 2006. doi:10.1088/0741-3335/48/5/005.

[14] N. Miyato et al. *Physics of Plasmas*, 11, 2004. doi: 10.1063/1.1811088.

[15] T. Dannert and F. Jenko. *Physics of Plasmas*, 12, 2005. doi:10.1063/1.1947447.

[16] P. Donnel et al. *Computer Physics Communications*, 234, 2019. doi:10.1016/j.cpc.2018.08.008.

[17] K. C. Shaing and S. P. Hirshman. *Physics of Fluids B: Plasma Physics*, 1, 1989. doi:10.1063/1.859134.

[18] K. C. Shaing et al. *Physics of Fluids B: Plasma Physics*, 4, 1992. doi:10.1063/1.860290.

[19] S. P. Hirshman. *The Physics of Fluids*, 21, 1978. doi: 10.1063/1.862195.

[20] S. P. Hirshman. *Nucl. Fusion*, 18, 1978. doi: 10.1088/0029-5515/18/7/004.

[21] J. D. Callen et al. *Physics of Plasmas*, 16, 2009. doi: 10.1063/1.3206976.

[22] G. Dif-Pradalier et al. *Physics of Plasmas*, 18, 2011. doi: 10.1063/1.3592652.

[23] Y. Sarazin et al. *Plasma Phys. Control. Fusion*, 63, 2021. doi:10.1088/1361-6587/abf673.

[24] C. C. Petty et al. *Physics of Plasmas*, 11, 2004. doi: 10.1063/1.1645791.

[25] M. Ottaviani et al. *Plasma Phys. Control. Fusion*, 39, 1997. doi:10.1088/0741-3335/39/9/012.

[26] R. Varennes et al. *Phys. Rev. Lett.*, 128, 2022. doi: 10.1103/PhysRevLett.128.255002.

[27] R. E. Waltz et al. *Physics of Plasmas*, 14, 2007. doi: 10.1063/1.2824376.

[28] R. Varennes et al. *Plasma Phys. Control. Fusion*, 2023. doi:10.1088/1361-6587/acb79a.

[29] T. A. Gianakon et al. *Physics of Plasmas*, 9, 2002. doi: 10.1063/1.1424924.

[30] P. Helander and D. J. Sigmar. Cambridge Monographs on Plasma Physics. 2005.